Author Manuscript

Author Manuscript

Author Manuscript

Author Manuscript

HHS Public Access

Author manuscript

Clin Neuroradiol. Author manuscript; available in PMC 2021 September 01.

Published in final edited form as:

Clin Neuroradiol. 2020 September ; 30(3): 581–589. doi:10.1007/s00062-019-00814-z.

Age-related Brain Metabolic Changes up to Seventh Decade in Healthy Humans:

Whole-brain Magnetic Resonance Spectroscopic Imaging Study

Helen Maghsudi[1], **Martin Schütze**[1], **Andrew A. Maudsley**[2], **Mete Dadak**[1], **Heinrich Lanfermann**[1], **Xiao-Qi Ding**[1]

[1]Institute of Diagnostic and Interventional Neuroradiology, Hannover Medical School, Carl-Neuberg-Str. 1, 30625 Hannover, Germany

[2]Department of Radiology, University of Miami School of Medicine, Miami, FL, USA

Abstract

Purpose—To study brain metabolic changes under normal aging and to collect reference data for the study of neurodegenerative diseases.

Methods—A total of 55 healthy subjects aged 20–70 years ($n \geq 5$ per age decade for each gender) underwent whole-brain magnetic resonance spectroscopic imaging at 3T after completing a DemTect test and the Beck depressions inventory II to exclude cognitive impairment and mental disorder. Regional concentrations of N–acetylaspartate (NAA), choline-containing compounds (Cho), total creatine (tCr), glutamine and glutamate (Glx), and myo-inositol (mI) were determined in 12 brain regions of interest (ROIs). The two-sided t-test was used to estimate gender differences and linear regression analysis was carried out to estimate age dependence of brain regional metabolite contents.

Results—Brain regional metabolite concentrations changed with age in the majority of selected brain regions. The NAA decreased in 8 ROIs with a rate varying from −4.9% to −1.9% per decade, reflecting a general reduction of brain neuronal function or volume and density in older age; Cho increased in 4 ROIs with a rate varying from 4.3% to 6.1%; tCr and mI increased in one ROI (4.2% and 8.2% per decade, respectively), whereas Glx decreased in one ROI (–5.1% per decade), indicating an inhomogeneous increase of cell membrane turnover (Cho) with altered energy metabolism (tCr) and glutamatergic neuronal activity (Glx) as well as function of glia cell (mI) in normal aging brain.

Conclusion—Healthy aging up to the seventh decade of life is associated with regional dependent alterations of brain metabolism. These results provide a reference database for future studies of patients.

Helen Maghsudi, maghsudi.helen@mh-hannover.de.

Conflict of interest H. Maghsudi, M. Schütze, A.A. Maudsley, M. Dadak, H. Lanfermann and X.-Q. Ding declare that they have no competing interests.

Electronic supplementary material The online version of this article (https://doi.org/10.1007/s00062-019-00814-z) contains supplementary material, which is available to authorized users.

Author Manuscript Author Manuscript Author Manuscript Author Manuscript

Keywords

Healthy aging; Human brain metabolites; Whole-brain MR spectroscopic imaging

Introduction

Knowledge of brain metabolic changes under normal aging is a prerequisite for identiffcation of pathological metabolic alterations caused by neurodegenerative processes. Proton magnetic resonance spectroscopy (^{1}H-MRS) detectable brain metabolites, e.g. N-acetylaspartate and N-acetylaspartylglutamate (NAA), choline-containing compounds (Cho), creatine and phosphocreatine (tCr), glutamate and glutamine (Glx), and myo-inositol (mI), provide information about neuronal density and integrity (NAA), turnover of cell membranes (tCho), energy metabolism (tCr), glutamatergic neuronal activity (Glx) and brain cell activity related to glia cell or osmolality (mI) [1]. Therefore, ^{1}H-MRS has been widely used to study aging human brains [2–6]; however, due to limitations of commonly used single voxel spectroscopy (SVS) or 2 dimensional (2D) MRS, the majority of previous ^{1}H-MRS studies measured metabolite changes in one or a few small brain regions [7, 8], which may not reflect the metabolic status of the whole aging brain. A recently established whole-brain ^{1}H-spectroscopic imaging (wbMRSI) technique has shown the potential for determination of brain metabolites over large coverage [5, 6, 9, 10] or in multiple small brain regions [11] with comparable quality to those measured using conventional SVS [12], enabling a spatial overview of regional metabolic changes within the whole brain under aging. Such information might provide not only reference data for identification of pathological alterations in patients but also contribute to understanding of the findings observed by other studies. These showed that the brain functions as organized networks with interactions between different brain regions and shows resting state functional connectivity, while aging affects brain networks inhomogeneously with high-order cognitive networks being more impaired, and the metabolic alterations may compromise brain functional connectivity [13–16]; however, in spite of numerous studies, the data reporting metabolic changes measured simultaneously in multiple specific brain regions, especially those including metabolites with small MRS signals (e.g. Glx or mI), are still rare. Therefore, in this study a short echo-time (TE) wbMRSI has been used to examine metabolic alterations associated with normal aging by determination of NAA, Cho, tCr, Glx, and mI contents in multiple different brain areas.

Methods

Subjects

The study was approved by the local institutional review board and written consent was obtained from all subjects. Healthy volunteers were recruited from the local population. After receiving a complete description of the study each participant was interviewed for health history and completed two screening tests to exclude cognitive or psychiatric impairments, the DemTect and the Beck depressions inventory revision [17, 18]. Exclusion criteria were current or past neurological or psychiatric disorder, current physical disorder, chronic arterial hypertension, diabetes, a past history of brain trauma, cardiometabolic or

Author Manuscript Author Manuscript Author Manuscript Author Manuscript

autoimmune disorders, obesity as well as subjects with abnormal results of the screening tests or abnormal MR morphological findings. Finally, 55 subjects aged between 20–70 years (mean age 44 ± 15 years, 27 males of mean age 43 ± 15 and 28 females of mean age 44 ± 15 years, for both genders $n \geq 5$ per age decade) were included. Of the subjects 11 were excluded due to abnormal screening tests ($n = 4$), obesity ($n = 5$) or incomplete MR examinations ($n = 2$).

MR Examinations and Data Processing

The MR examinations were carried out at 3T (Verio, Siemens, Erlangen, Germany). A 12-channel phased-array head coil was used. The MRI protocol included a T2-weighted turbo spin echo (TSE) sequence, a T2-weighted gradient (GRE) echo sequence, a fluid attenuation inversion recovery (FLAIR) sequence, a T1-weighted 3D magnetization-prepared rapid gradient echo (MPRAGE) sequence, and a volumetric spin-echo planar spectroscopic imaging (EPSI) acquisition (TR/TE= 1550/17.6ms, field of view 280× 280× 180mm^3 and a slab of 140mm) as described previously for wbMRSI, with a nominal basic voxel volume of approximately 1.5ml following spatial smoothing [6, 19]. The EPSI acquisition included a second dataset obtained without water suppression (water reference MRSI) that provided a water reference signal with identical spatial parameters to the metabolite MRSI. The water reference MRSI was used for several processing functions, including measurement and correction of the resonance frequency offset at each voxel location, correction of line shape distortions and to provide internal signal reference for the normalization of metabolite concentrations [20], while the MPRAGE images were used as anatomical references. The EPSI, MPRAGE, FLAIR, TSE and GRE scans were obtained with the same angulation, so that the same anatomical structures could be identified. The FLAIR, T2 and T1 weighted images were inspected by two experienced neuroradiologists to recognize possible morphological abnormalities.

The EPSI data were analyzed by using the software package Metabolic Imaging and Data Analysis System (MIDAS) (mrir.med.miami.edu:8000/midas/) as described previously [19, 21, 22] to obtain volumetric brain maps of NAA, Cr, tCho, Glx, mI and spectral line width, which included lipid k-space extrapolation, spectral line shape and B0 correction, and parametric spectral analysis using Gaussian line shape for fitting signals from the metabolites. The voxels were excluded from the spectral fitting if the line width of the water signal at the corresponding voxel exceeded 15Hz. The processing also included calculation of the relative tissue volume contribution to each MRSI voxel, by applying a tissue segmentation procedure with FMRIB's software library (FSL) (fsl.fmrib.ox.ac.uk/fsl/fslwiki/) [23] to the T1-weighted MPRAGE data to map grey matter (GM), white matter (WM) and cerebrospinal fluid (CSF). This is followed by a resampling and convolution by the MRSI spatial response function to coincide with the MRSI voxel volume and location, resulted in fractional volume maps of brain tissue (FVBT) and cerebrospinal fluid (FVCSF) [19, 22]. The metabolite images were reconstructed to 64× 64× 32 points with the nominal voxel volume of 0.31ml that was increased to approximately 1.5ml following spatial smoothing. A nonlinear spatial transform was used to transform all resultant maps to a standard spatial reference, which included interpolation to 2mm isotropic voxels [22, 24].

Author Manuscript Author Manuscript Author Manuscript Author Manuscript

Decade mean metabolite maps were derived by averaging the maps of the subjects within corresponding age decade.

Regions of Interest Analysis

Brain metabolite concentrations [NAA], [tCho], [tCr], [Glx], and [mI] (normalized in reference to internal water, and presented in institutional unit, i.u.), together with the spectral linewidths, were determined on the corresponding brain maps by using mean values over selected regions of interest (ROIs). A total of 12 ROIs were chosen within each brain hemisphere, where they are potentially preferably affected by different diseases with respect to future studies on patients: two ROIs located in the cerebellum—hemisphere of cerebellar anterior lobe at the level between pons and mesencephalon (Cbla) and cerebellar white matter at level of middle cerebellar peduncle (Cblwm), two ROIs in mid-brain—tegmentum (MDd) and cerebral peduncle (MDv) and 8 ROIs in the cerebrum—centrum semiovale (CSO), frontal white matter (fWM), subcortical hand motor area (HN), posterior limb of the internal capsule (iCap), putamen, parietal white matter (pWM), splenium of the corpus callosum (SCC) and thalamus. Due to local magnetic field distortions caused by neighboring structures containing bone and air no ROIs were selected at genu of the corpus callosum and caudate nucleus. All ROIs were selected carefully in referenced T1-weighted images according to anatomical landmarks to minimize partial volume effects, and the values were measured with an area of $26mm^2$ on a single slice of corresponding metabolite maps by using the ROI tool integrated in MIDAS. As quality controls, metabolite values obtained with a linewidth larger than 14Hz or with a signal-to-noise ratio (S/N, derived as ratio of the mean value over the ROI to the standard deviation) less than 4 were not sampled. Considering sample size limitations related to the handedness ($n = 49$ for right hand vs. 6 for left hand), the values of corresponding ROIs in left and right hemispheres were averaged for further analysis, where the values of only one hemisphere ROI were used when those of corresponding ROI in other hemisphere were excluded due to broad linewidth or smaller SNR. Corrections for cerebrospinal fluid (CSF) volume contributions to ROI measurements were applied as Met' = Met/(1-FVcsf), where FVcsf was the fractional volume of CSF within each ROI. Decade mean values of [NAA], [Cho], [tCr], [Glx], and [mI] of the healthy volunteers at each ROI were derived by averaging corresponding values of the subjects within the age decade.

Statistical Analysis

Normal distributions of the data were verified by Shapiro-Wilk tests and quantile-quantile plots. The two-sided t-tests with Bonferroni corrected significance level ($\alpha = 0.05 /6 \times 12 \approx 0.0007$) were performed to estimate gender differences of measured brain metabolite concentrations and spectral linewidth. One-way ANOVA trend analysis was used to estimate relationships between age and the measured metabolite concentrations, which did not reveal significant quadratic or higher order relationships ($p > 0.05$). Therefore, linear regression analysis with a significance level $\alpha = 0.05 /6 \approx 0.008$ that was corrected for multiple linear regression analyses at each ROI was used to estimate the age dependence of brain regional metabolite concentrations and the spectral linewidth, where the results with $p < \alpha$ were considered as showing significant age dependence, those with $\alpha < p < 0.05$ as not significant but showing a tendency of age dependence. Statistical analyses were performed with SPSS

Author Manuscript Author Manuscript Author Manuscript Author Manuscript

version 24 (SPSS IBM, Armonk, NY, USA), and graphic displays were made by using software Origin (OriginLab, Northampton, MA, USA).

Results

Example mean maps of NAA, Cho, tCr, Glx and mI of the third decade derived from subjects aged between 21–30 years ($n = 12$, Fig. 1a) and those of the seventh decade derived from subjects aged between 61–70 years ($n = 11$, Fig. 1b) are shown in Fig. 1, which provides a brief overview about the differences of brain metabolite contents in youngest and oldest subjects in this study. The overall signal intensities in NAA maps of the seventh decade are much weaker than those of the third decade, demonstrating a decrease of brain NAA contents in old subjects, while the differences of the signal intensities of the other metabolites between both age decades are not so distinct. In Fig. 2 the locations of the 12 ROIs are shown in the right brain hemisphere as white filled circles on T1-weighted images from a volunteer (male, 52 years) (Fig. 2a), as well as example MR spectra in each of the ROIs in cerebellum or cerebrum as indicated (Fig. 2b). The two-sided t-tests did not reveal significant gender difference for all measured metabolite contents ($p > 0.0007$). Therefore, in the following analyses the values of males and females were combined. The decade mean values of [NAA], [Cho], [tCr], [Glx], [mI], and corresponding spectral linewidths in each brain ROI are given in Online Resource 1. Note that due to the application of the data quality criteria $S/N \geq 4$ in certain ROIs not all subjects' values were sampled.

While the significant results of linear regression analysis are summarized in Table 1, the linear fits to age for the ROIs with significant ($p < 0.008$) or tendency ($0.008 < p < 0.05$) correlations, together with the 95% confidence bands of the fits, are shown in Fig. 3. As observable in Table 1 and Fig. 3, the linear regression analysis revealed that the measured metabolite concentrations and spectral linewidths correlated significantly with age at certain ROIs: [NAA] decreased significantly with age in the ROIs MDd, fWM, iCap and putamen (correlation coefficient R = −0.37 to −0.53, $p < 0.008$), and with a tendency in the ROIs MDv, HN, pWM, and thalamus (R = −0.27 to −0.33, $p < 0.05$). The change rate of [NAA] varied from −4.9% (putamen) to −1.9% (HN) per decade (Fig. 3a). The [Cho] increased with age significantly in HN and iCap (R = 0.38–0.40, $p < 0.008$) and with a tendency in CSO and sCC (R = 0.32–0.34, $0.008 < p < 0.05$), with a rate varying from 4.3% (CSO) to 6.1% (HN) per decade. There was a trend to increased [tCr] (R = 0.35, 4.2% per decade) and significantly increased [mI] (R = 0.37, 8.2% per decade) in the same ROI (CSO), whereas [Glx] decreased significantly in thalamus (R = −0.43, −5.1% per decade) (Fig. 3b). The linewidth revealed significant age-dependent increases in 6 ROIs (Cbla, CSO, HN, putamen, sCC, and thalamus, R = 0.38–0.49, $p < 0.008$) and with a tendency in pWM (R = 0.27, $p = 0.049$), with a rate varying from 3.4% (pWM) to 7.4% (hand motor area) per decade. The cerebellar ROIs (Cbla and Cblwm) did not show age-related metabolite changes, while an age-related increase of linewidth in Cbla was observed (Fig. 3c).

Discussion

In this study, based on a wbMRSI scan with an acquisition time of about 16min, brain metabolite concentrations were determined by post-processing in 12 different structures of

Author Manuscript Author Manuscript Author Manuscript Author Manuscript

aging human brain. The derived mean concentrations of NAA, Cho, tCr, Glx and mI, in reference to internal water signal, are in agreement with those in adult human brain reported previously by Pouwels and Frahm, who studied healthy volunteers by using 8 SVS in the cerebrum and 2 SVS in the cerebellum, with an acquisition time of about 6min for each SVS [3]. This again proves that simultaneous metabolite measurements in multiple brain regions by using wbMRSI acquisition are as reliable as those derived with conventional SVS, with additional advantages of reduced burden for subjects and more efficiency for clinicians by shortening total MR examination time. The obtained metabolite values may provide a reference for future studies on metabolic alterations in patients.

The major findings of the study are the age-related regional inhomogeneous changes of metabolite concentrations in aging human brain. As shown in Table 1, metabolite concentrations changed significantly with age in multiple brain structures, with a rate differing by metabolites and brain regions: [NAA] decreased in 8 out of 12 ROIs, with the largest change occurring in putamen (–4.9% per decade), then in midbrain tegmentum (–3.8% per decade), frontal white matter (–3.7% per decade), and the lowest rate in HN (–1.9% per decade). Comparatively, Cho, tCr, Glx and mI showed less age-related changes: [Cho] increased with age in 4 out of 12 ROIs that were located mainly along pyramidal tracts (HN, CSO, and iCap), most rapidly in HN (6.1% per decade) and slowest in SCC (3.2% per decade), whereas tCr, Glx and mI showed age-related changes only in 1 out of 12 ROIs, i.e. both [tCr] and [mI] increased with age in CSO (4.2% and 8.2% per decade, respectively), and [Glx] decreased with age in thalamus (–5.1% per decade). Therefore, the present results of simultaneous MRS measurements in multiple brain regions revealed the inhomogeneous spatial allocations of metabolic aging within the human brain.

Age-related changes of brain metabolite concentrations have been reported previously in numerous MRS studies. A decrease of brain NAA with age has been observed in a majority of the studies [5–8]. Consistent with those reported previously, the present findings of decreased [NAA] with age in the majority of selected brain structures indicate that an age-related decrease of NAA is a main metabolic aging process within the human brain. In line with histological findings that the total number of neurons decreased with age [25] and structural MRI findings of decreased gray matter volume with age [26, 27], age-related decrease of NAA has been deduced to decrease neuronal volume or density and neuronal function [2, 6, 28, 29]. Correspondingly, the present observations that [NAA] decreased with age more rapidly in putamen, tegmentum and frontal white matter than in other brain areas may indicate more rapid decreases of neuronal volume and function in these brain structures, which may be the possible reason for these brain areas to be more frequently involved in pathological neurodegeneration [30, 31], i.e. aging seems to be a primary risk factor for neurodegenerative diseases, which was also reported by studies on non-human primates [32].

Previous findings regarding changes of Cho and tCr with age are more varied [5, 11, 28, 33–35], and only a few studies reported changes of Glx and mI contents in aging human brains [34–37]. For example, Raininko and Mattsson in a SVS (TR /TE= 6000/22ms) study at 1.5T on 57 subjects aged 13–72 years (25 women) found no age dependence for [Cho] and [tCr] but increased [mI] with age, while the highest [Glx] was found in the youngest and oldest

Author Manuscript Author Manuscript Author Manuscript Author Manuscript

subjects in cerebral supraventricular white matter [34]. Charles et al. used MRSI (TR /TE= 2000/272ms) on 34 subjects aged 21–75 years (19 women) at 1.5T and found lower [Cho], and [tCr] in cortical and subcortical gray matter of older subjects but not in the white matter [2]. Brooks et al. found by using SVS at 1.5T on 50 healthy subjects aged 20–70 years that the concentrations of tCr and Cho did not change significantly with age in the frontal lobe [28]. By using similar multiple regional measurements but a wbMRSI with long echo time Eylers et al. found decreased [tCr] in the pons and putamen but no significant changes of [Cho] with age [11]. Consistent with the present findings of age-related increase of Cho, tCr and mI, and decrease of Glx Reyngoudt et al. studied 90 subjects (42 women and 48 men aged 18–76 years) with SVS in posterior cingulate cortex (PCC) and hippocampus (HC), and reported age-related increases of tCr and mI in the PCC, and increase of mI in the HC [35]. Using a 2D MRSI measurement, Gruber et al. reported increased Cho, tCr and mI with age in centrum semiovale [38]. Increased Cho, tCr, and mI concentrations and decreased Glx concentrations with age were also found in large scale brain structures [5, 6]. The reasons for divergent reports for age-related Cho, tCr, Glx, and mI, may not only be due to different acquisition techniques and different subject samples in these studies, but possibly also due to different targeted brain structures with inhomogeneous metabolic features, as reflected by varying regional metabolite concentrations and their age dependences (Table 1 and Fig. 3). Based on knowledge from studies of animal models the age-related increases of [Cho] may be interpreted as altered cellular membrane turnover, e.g. building up altered myelin sheaths due to ongoing, albeit inadequate, reparative myelination processes in aging brain [39, 40]. Accordingly, the present findings that the ROIs along pyramidal tracts (HN, CSO, and iCap) showed the most age-related [Cho] increases may indicate an age-related increase of such ongoing, albeit inadequate, reparative myelination process especially along the pyramidal tracts, which might be a compensatory alteration in healthy old people to balance motor function. Similarly, the increase of [tCr] could be considered as a compensatory alteration of the energy supply and neuroprotection [41], and the increased [mI] as altered gliosis [35]. The Glx signal combines glutamine and glutamate, with glutamate being the largest component and the major excitatory neurotransmitter of the central nervous system. Therefore, the decrease of [Glx] with age in thalamus may suggest a decrease of glutamatergic neuronal activity in old subjects. The observed significant age-related increase of the spectral linewidth in 7 ROIs is consistent with a previous study [5], and may be due to increased iron concentrations [42] and shorter metabolite T2 relaxation times in older subjects [43, 44] in these brain structures.

Limitations of the study include that possible changes of internal water content with age, which has been previously suggested [28, 45], were not considered, which would impact the measured metabolite concentrations, since it was used as reference for the metabolite signal normalization for all subjects. The results of Neeb et al. [46] indicated that between the third and eighth decades of life the changes of brain water content with age are relatively small and less than the variability between the subjects, and that the decrease of brain water content with age may only be a factor for gray matter in males over ~55 years old and is less than 5% at the age of 70 years. As an echo time of 17.6ms has been used that was much shorter than the T2 relaxation times of the metabolites NAA, tCr and tCho [43, 47], and the metabolites Glx and mI showed age-related changes only in one brain area, the

Author Manuscript Author Manuscript Author Manuscript Author Manuscript

measurements did not account for possible differences in water or metabolite T2 relaxation rates between subjects or with age. In addition, we did not consider differences between left and right hemispheres and the possible effect of handedness due to limited sample size, and subjects older than 70 years were not included due to difficulties in subject recruitment.

In conclusion, this study has demonstrated that healthy aging up to the seventh decade of life is associated with spatial inhomogeneous alterations of brain metabolite contents, which may contribute to an understanding of the origin of pathological neurodegeneration. The metabolite concentrations determined in healthy aging human brains may provide a reference database for future study of patients, which will be available on demand for interested scientists and clinicians.

Grant support

This work was partially supported by Deutsche Forschungsgemeinschaft (X.-Q. Ding) and by National Institutes of Health [grant number R01 EB016064] (A.A.M.).

References

1. Barker PB, Bizzi A, De Stefano N, Gullapalli RP, Lin DDM. Clinical MR Spectroscopy: Techniques and Applications. Cambridge: Cambridge University Press; 2010.
2. Charles HC, Lazeyras F, Krishnan KR, Boyko OB, Patterson LJ, Doraiswamy PM Proton spectroscopy of human brain: effects of age and sex. Prog Neuropsychopharmacol Biol Psychiatry. 1994;18:995–1004. [PubMed: 7824764]
3. Pouwels PJ, Frahm J. Regional metabolite concentrations in human brain as determined by quantitative localized proton MRS. Magn Reson Med. 1998;39:53–60. [PubMed: 9438437]
4. Chiu PW, Mak HK, Yau KK, Chan Q, Chang RC, Chu LW. Metabolic changes in the anterior and posterior cingulate cortices of the normal aging brain: proton magnetic resonance spectroscopy study at 3T. Age (Dordr). 2014;36:251–64. [PubMed: 23709317]
5. Maudsley AA, Govind V, Arheart KL. Associations of age, gender and body mass with 1H MR-observed brain metabolites and tissue distributions. NMR Biomed. 2012;25:580–93. [PubMed: 21858879]
6. Ding XQ, Maudsley AA, Sabati M, Sheriff S, Schmitz B, Schütze M, Bronzlik P, Kahl KG, Lanfermann H. Physiological neuronal decline in healthy aging human brain—An in vivo study with MRI and short echo-time whole-brain H MR spectroscopic imaging. Neuroimage. 2016;137:45–51. [PubMed: 27164326]
7. Haga KK, Khor YP, Farrall A, Wardlaw JM. A systematic review of brain metabolite changes, measured with 1H magnetic resonance spectroscopy, in healthy aging. Neurobiol Aging. 2009;30:353–63. [PubMed: 17719145]
8. Cleeland C, Pipingas A, Scholey A, White D. Neurochemical changes in the aging brain: A systematic review. Neurosci Biobehav Rev. 2019;98:306–19. [PubMed: 30625337]
9. Maudsley AA, Domenig C, Ramsay RE, Bowen BC. Application of volumetric MR spectroscopic imaging for localization of neocortical epilepsy. Epilepsy Res. 2010;88:127–38. [PubMed: 19926450]
10. Donadieu M, Le Fur Y, Lecocq A, Maudsley AA, Gherib S, Soulier E, Confort-Gouny S, Pariollaud F, Ranjeva MP, Pelletier J, Guye M, Zaaraoui W, Audoin B, Ranjeva JP. Metabolic voxel-based analysis of the complete human brain using fast 3D-MRSI: Proof of concept in multiple sclerosis. J Magn Reson Imaging. 2016;44:411–9. [PubMed: 26756662]
11. Eylers VV, Maudsley AA, Bronzlik P, Dellani PR, Lanfermann H, Ding XQ. Detection of normal aging effects on human brain metabolite concentrations and microstructure with whole-brain MR spectroscopic imaging and quantitative MR imaging. AJNR Am J Neuroradiol. 2016;37:447–54. [PubMed: 26564440]

Author Manuscript Author Manuscript Author Manuscript Author Manuscript

12. Maghsudi H, Schmitz B, Maudsley AA, Sheriff S, Bronzlik P, Schütze M, Lanfermann H, Ding X. Regional Metabolite Concentrations in Aging Human Brain: Comparison of Short-TE Whole Brain MR Spectroscopic Imaging and Single Voxel Spectroscopy at 3T. Clin Neuroradiol. 2019 1 18. doi: 10.1007/s00062-018-00757-x. [Epub ahead of print]
13. Damoiseaux JS, Beckmann CF, Arigita EJ, Barkhof F, Scheltens P, Stam CJ, Smith SM, Rombouts SA. Reduced resting-state brain activity in the "default network" in normal aging. Cereb Cortex. 2008;18:1856–64. [PubMed: 18063564]
14. Siman-Tov T, Bosak N, Sprecher E, Paz R, Eran A, Aharon-Peretz J, Kahn I. Early Age-Related Functional Connectivity Decline in High-Order Cognitive Networks. Front Aging Neurosci. 2017;8:330. [PubMed: 28119599]
15. Madden DJ, Parks EL, Tallman CW, Boylan MA, Hoagey DA, Cocjin SB, Packard LE, Johnson MA, Chou YH, Potter GG, Chen NK, Siciliano RE, Monge ZA, Honig JA, Diaz MT. Sources of disconnection in neurocognitive aging: cerebral white-matter integrity, resting-state functional connectivity, and white-matter hyperintensity volume. Neurobiol Aging. 2017;54:199–213. [PubMed: 28389085]
16. Johnson B, Zhang K, Gay M, Neuberger T, Horovitz S, Hallett M, Sebastianelli W, Slobounov S. Metabolic alterations in corpus callosum may compromise brain functional connectivity in MTBI patients: an 1H-MRS study. Neurosci Lett. 2012;509:5–8. [PubMed: 22108503]
17. Steer RA, Clark DA, Beck AT, Ranieri WF. Common and specific dimensions of self-reported anxiety and depression: the BDI-II versus the BDI-IA. Behav Res Ther. 1999;37:183–90. [PubMed: 9990749]
18. Kalbe E, Kessler J, Calabrese P, Smith R, Passmore AP, Brand M, Bullock R. DemTect: a new, sensitive cognitive screening test to support the diagnosis of mild cognitive impairment and early dementia. Int J Geriatr Psychiatry. 2004;19:136–43. [PubMed: 14758579]
19. Ding XQ, Maudsley AA, Sabati M, Sheriff S, Dellani PR, Lanfermann H. Reproducibility and reliability of short-TE whole-brain MR spectroscopic imaging of human brain at 3T. Magn Reson Med. 2015;73:921–8. [PubMed: 24677384]
20. Barker PB, Soher BJ, Blackband SJ, Chatham JC, Mathews VP, Bryan RN. Quantitation of proton NMR spectra of the human brain using tissue water as an internal concentration reference. NMR Biomed. 1993;6:89–94. [PubMed: 8384470]
21. Maudsley AA, Darkazanli A, Alger JR, Hall LO, Schuff N, Studholme C, Yu Y, Ebel A, Frew A, Goldgof D, Gu Y, Pagare R, Rousseau F, Sivasankaran K, Soher BJ, Weber P, Young K, Zhu X. Comprehensive processing, display and analysis for in vivo MR spectroscopic imaging. NMR Biomed. 2006;19:492–503. [PubMed: 16763967]
22. Maudsley AA, Domenig C, Govind V, Darkazanli A, Studholme C, Arheart K, Bloomer C. Mapping of brain metabolite distributions by volumetric proton MR spectroscopic imaging (MRSI). Magn Reson Med. 2009;61:548–59. [PubMed: 19111009]
23. Smith SM, Jenkinson M, Woolrich MW, Beckmann CF, Behrens TE, Johansen-Berg H, Bannister PR, De Luca M, Drobnjak I, Flit-ney DE, Niazy RK, Saunders J, Vickers J, Zhang Y, De Stefano N, Brady JM, Matthews PM. Advances in functional and structural MR image analysis and implementation as FSL. Neuroimage. 2004;23 Suppl 1:S208–19. [PubMed: 15501092]
24. Collins DL, Zijdenbos AP, Kollokian V, Sled JG, Kabani NJ, Holmes CJ, Evans AC. Design and construction of a realistic digital brain phantom. IEEE Trans Med Imaging. 1998;17:463–8. [PubMed: 9735909]
25. Pakkenberg B, Gundersen HJ. Neocortical neuron number in humans: effect of sex and age. J Comp Neurol. 1997;384:312–20. [PubMed: 9215725]
26. Bartzokis G, Beckson M, Lu PH, Nuechterlein KH, Edwards N, Mintz J. Age-related changes in frontal and temporal lobe volumes in men: a magnetic resonance imaging study. Arch Gen Psychiatry. 2001;58:461–5. [PubMed: 11343525]
27. Hasan KM, Walimuni IS, Kramer LA, Frye RE. Human brain atlas-based volumetry and relaxometry: application to healthy development and natural aging. Magn Reson Med. 2010;64:1382–9. [PubMed: 20740662]

Author Manuscript Author Manuscript Author Manuscript Author Manuscript

28. Brooks JC, Roberts N, Kemp GJ, Gosney MA, Lye M, White-house GH. A proton magnetic resonance spectroscopy study of age-related changes in frontal lobe metabolite concentrations. Cereb Cortex. 1991;11:598–605.
29. Chao LL, Mueller SG, Buckley ST, Peek K, Raptentsetseng S, Elman J, Yaffe K, Miller BL, Kramer JH, Madison C, Mungas D, Schuff N, Weiner MW. Evidence of neurodegeneration in brains of older adults who do not yet fulfill MCI criteria. Neurobiol Aging. 2010;31:368–77. [PubMed: 18550226]
30. Lin SC, Lin KJ, Hsiao IT, Hsieh CJ, Lin WY, Lu CS, Wey SP, Yen TC, Kung MP, Weng YH. In vivo detection of monoaminergic degeneration in early Parkinson disease by (18)F-9-fluoropropyl-(+)-dihydrotetrabenzazine PET. J Nucl Med. 2014;55:73–9. [PubMed: 24287322]
31. Firbank MJ, Harrison RM, O'Brien JT. A comprehensive review of proton magnetic resonance spectroscopy studies in dementia and Parkinson's disease. Dement Geriatr Cogn Disord. 2002;14:64–76. [PubMed: 12145453]
32. Collier TJ, Kanaan NM, Kordower JH. Ageing as a primary risk factor for Parkinson's disease: evidence from studies of non-human primates. Nat Rev Neurosci. 2011;12:359–66. [PubMed: 21587290]
33. Harada M, Miyoshi H, Otsuka H, Nishitani H, Uno M. Multivariate analysis of regional metabolic differences in normal ageing on localised quantitative proton MR spectroscopy. Neuroradiology. 2001;43:448–52. [PubMed: 11465755]
34. Raininko R, Mattsson P. Metabolite concentrations in supraventricular white matter from teenage to early old age: A short echo time 1H magnetic resonance spectroscopy (MRS) study. Acta Radiol. 2010;51:309–15. [PubMed: 20170295]
35. Reyngoudt H, Claeys T, Vlerick L, Verleden S, Acou M, Deblaere K, De Deene Y, Audenaert K, Goethals I, Achten E. Age-related differences in metabolites in the posterior cingulate cortex and hippocampus of normal ageing brain: a 1H-MRS study. Eur J Radiol. 2012;81:e223–31. [PubMed: 21345628]
36. Sailasuta N, Ernst T, Chang L. Regional variations and the effects of age and gender on glutamate concentrations in the human brain. Magn Reson Imaging. 2008;26:667–75. [PubMed: 17692491]
37. Tunc-Skarka N, Meier S, Demirakca T, Sack M, Weber-Fahr W, Brusniak W, Wolf I, Matthäus F, Schulze TG, Diener C, Ende G. Effects of normal aging and SCN1A risk-gene expression on brain metabolites: evidence for an association between SCN1A and myo-inositol. NMR Biomed. 2014;27:228–34. [PubMed: 24357141]
38. Gruber S, Pinker K, Riederer F, Chmelík M, Stadlbauer A, Bittsanský M, Mlynárik V, Frey R, Serles W, Bodamer O, Moser E. Metabolic changes in the normal ageing brain: consistent findings from short and long echo time proton spectroscopy. Eur J Radiol. 2008;68:320–7. [PubMed: 17964104]
39. Bowley MP, Cabral H, Rosene DL, Peters A. Age changes in myelinated nerve fibers of the cingulate bundle and corpus callosum in the rhesus monkey. J Comp Neurol. 2010;518:3046–64. [PubMed: 20533359]
40. Sandell JH, Peters A. Disrupted myelin and axon loss in the anterior commissure of the aged rhesus monkey. J Comp Neurol. 2003;466:14–30. [PubMed: 14515238]
41. Rae CD, Bröer S. Creatine as a booster for human brain function. How might it work? Neurochem Int. 2015;89:249–59. [PubMed: 26297632]
42. Mitsumori F, Watanabe H, Takaya N. Estimation of brain iron concentration in vivo using a linear relationship between regional iron and apparent transverse relaxation rate of the tissue water at 4.7T. Magn Reson Med. 2009;62:1326–30. [PubMed: 19780172]
43. Kirov II, Fleysher L, Fleysher R, Patil V, Liu S, Gonen O. Age dependence of regional proton metabolites T2 relaxation times in the human brain at 3T. Magn Reson Med. 2008;60:790–5. [PubMed: 18816831]
44. Marjańska M, Emir UE, Deelchand DK, Terpstra M. Faster metabolite (1)H transverse relaxation in the elder human brain. PLoS ONE. 2013;8:e77572. [PubMed: 24098589]
45. Christiansen P, Toft PB, Gideon P, Danielsen ER, Ring P, Henriksen O. MR-visible water content in human brain: a proton MRS study. Magn Reson Imaging. 1994;12:1237–44. [PubMed: 7854029]

Author Manuscript Author Manuscript Author Manuscript Author Manuscript

46. Neeb H, Zilles K, Shah NJ. Fully-automated detection of cerebral water content changes: study of age- and gender-related H2O patterns with quantitative MRI. Neuroimage. 2006;29:910–22. [PubMed: 16303316]

47. Jiru F, Skoch A, Wagnerova D, Dezortova M, Viskova J, Profant O, Syka J, Hajek M. The age dependence of T2 relaxation times of N-acetyl aspartate, creatine and choline in the human brain at 3 and 4T. NMR Biomed. 2016;29:284–92. [PubMed: 26752593]

Author Manuscript Author Manuscript Author Manuscript Author Manuscript

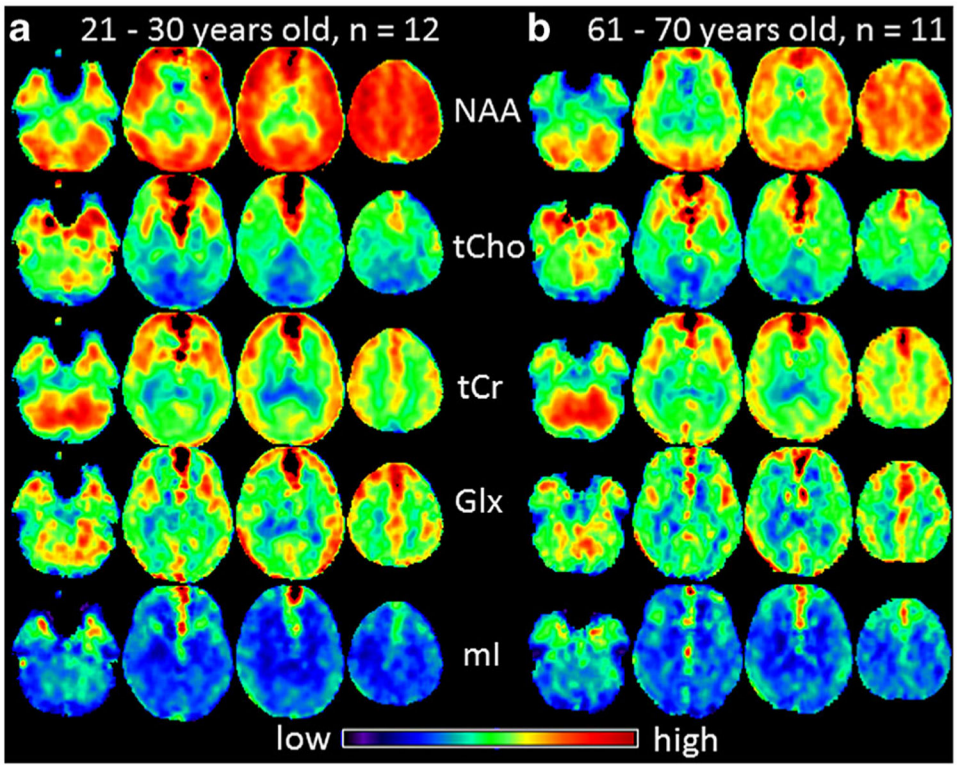

Fig. 1.

Example mean maps of NAA, tCho, tCr, Glx and mI averaged among subjects of the youngest group (21–30 years old, $n = 12$, **a**) and averaged among subjects of the oldest group (61–70 years old, $n = 11$, **b**), respectively, are shown. Due to local magnetic field distortions caused by neighboring structures containing bone and air there are some hyperintensive voxels with excessive linewidth, which were excluded in the ROI measurements

Author Manuscript Author Manuscript Author Manuscript Author Manuscript

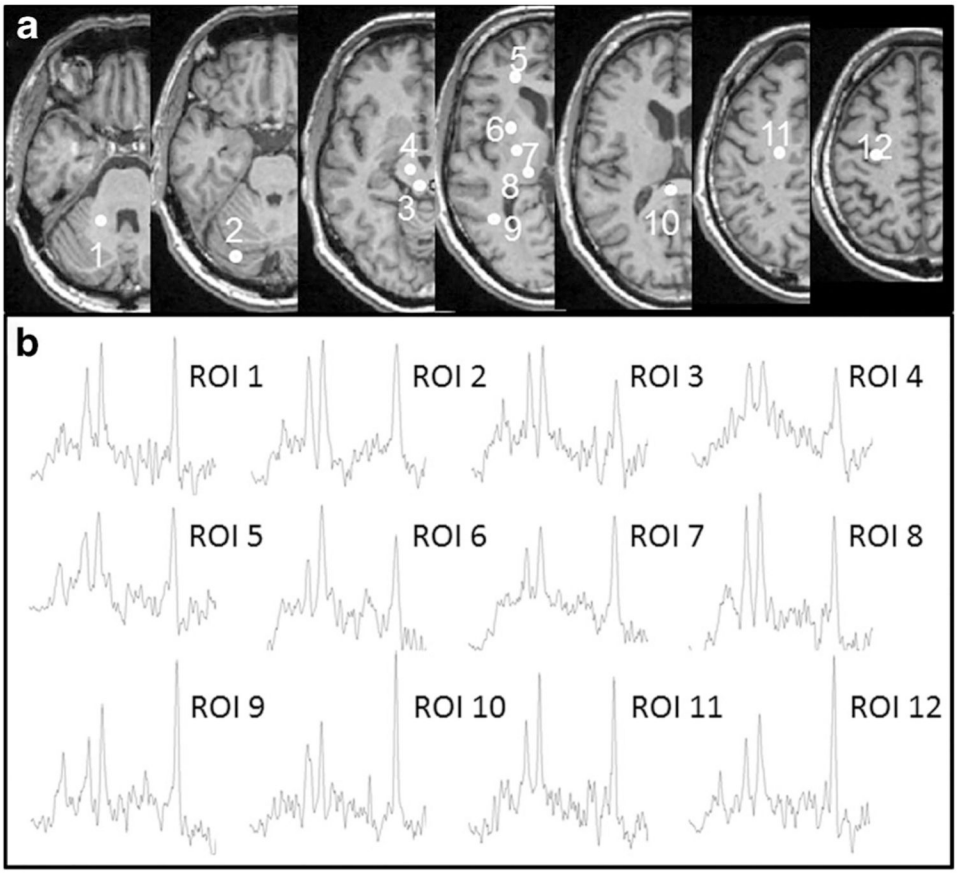

Fig. 2.

a Locations of selected regions of interest (ROIs) in the right brain hemisphere displayed as white filled circles on T1 weighted images of a volunteer (male, 52 years). The consecutive numbers represent the ROIs located in cerebellar white matter at level of middle cerebellar peduncle (Cblwm, *1*), cerebellar anterior lobe at level of pons (Cbla, *2*), midbrain tegmentum (MDd, *3*) and cerebral peduncle (MDv, *4*), frontal white matter (fWM, *5*), putamen (*6*), posterior limb of the internal capsule (iCap, *7*), thalamus (*8*), parietal white matter (pWM, *9*), splenium of the corpus callosum (sCC, *10*), centrum semiovale (CSO, *11*) and hand motor area (HN, *12*). **b** Example MR spectra in each of the ROIs in cerebellum and cerebrum as indicated, derived from whole-brain magnetic resonance spectroscopic imaging data

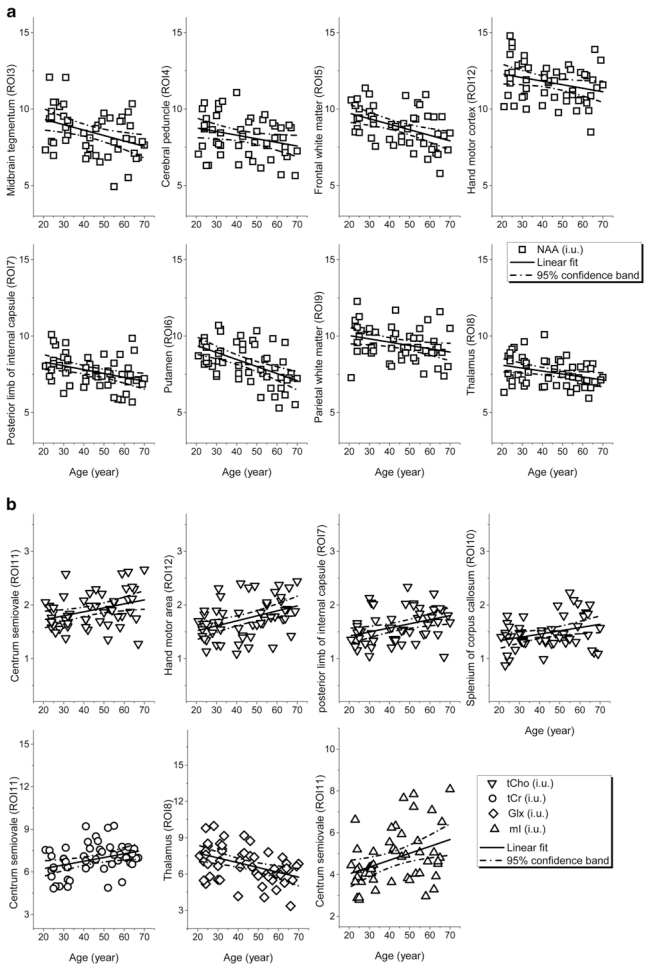

Author Manuscript Author Manuscript Author Manuscript Author Manuscript

Author Manuscript Author Manuscript Author Manuscript Author Manuscript

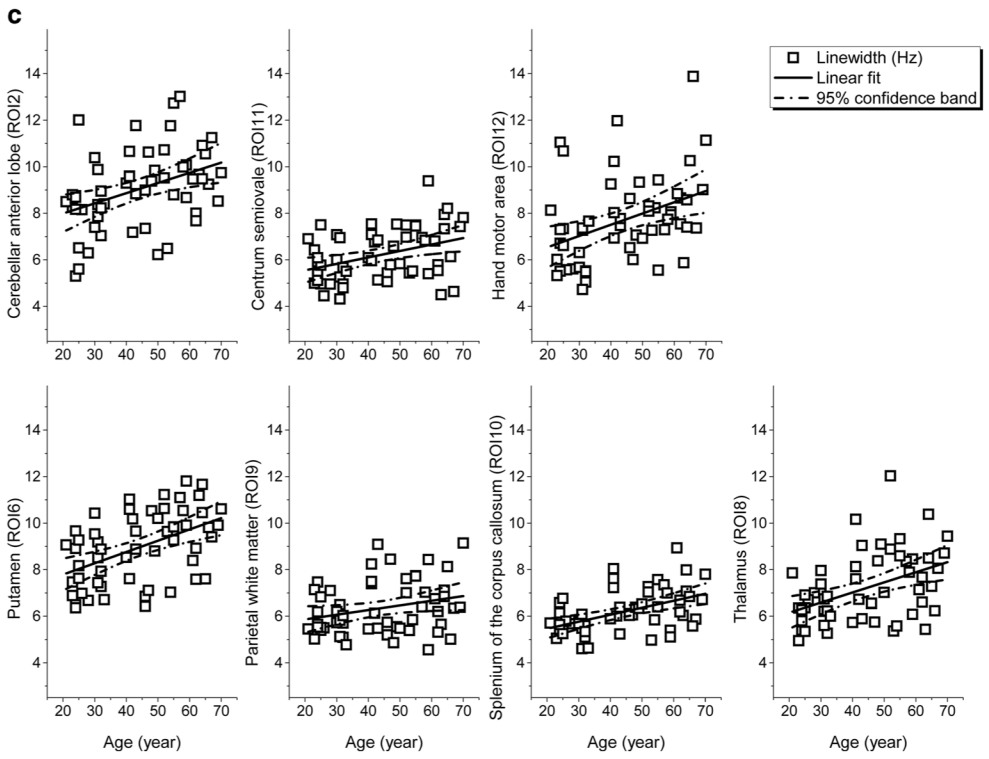

Fig. 3.

a Regional [NAA] of the ROIs that showed significant correlations ($p < 0.008$) to age and the linear fits to age together with corresponding 95% confidence bands plotted against age. **b** Regional [tCho], [tCr], [Glx], and [mI] of the ROIs that showed significant correlations ($p < 0.008$) to age and the linear fits to age together with corresponding 95% confidence bands plotted against age **c** Spectral linewidths of the ROIs that showed significant correlations ($p < 0.008$) to age and the linear fits to age together with corresponding 95% confidence bands plotted against age. All regional metabolite concentrations were measured in ratio to internal water, and present in institutional units (i.u.)

Author Manuscript Author Manuscript Author Manuscript Author Manuscript

Table 1

Significant linear age dependence of local brain metabolite concentrations and spectral linewidths

ROI	NAA			Intercept		Slope		Decade variation
	N	R	*p*	Value	SD	Value	SD	%
MDd	52	−0.375**	0.006	10.04	0.57	−0.035	0.012	−3.80
MDv	52	−0.281*	0.043	9.25	0.53	−0.024	0.011	−2.71
fWM	52	−0.446**	0.001	10.46	0.48	−0.036	0.010	−3.72
HN	54	−0.272*	0.046	12.75	0.53	−0.023	0.011	−1.89
iCap	55	−0.372**	0.005	8.81	0.40	−0.025	0.009	−3.03
Putamen	55	−0.531**	0.000	10.32	0.47	−0.046	0.010	−4.91
pWM	55	−0.298*	0.027	10.47	0.44	−0.022	0.009	−2.15
Thalamus	54	−0.328*	0.016	8.49	0.36	−0.019	0.008	−2.39
Cho								
CSO	53	0.342*	0.012	1.58	0.13	0.007	0.003	4.28
HN	55	0.394**	0.003	1.33	0.14	0.009	0.003	6.11
iCap	55	0.376**	0.005	1.27	0.12	0.008	0.003	5.37
SCC	53	0.316*	0.021	1.21	0.12	0.006	0.003	4.59
tCr								
CSO	52	0.349*	0.011	5.70	0.45	0.026	0.010	4.19
Glx								
Thalamus	53	−0.426**	0.001	8.52	0.55	−0.040	0.012	−5.13
ml								
CSO	50	0.370**	0.008	3.37	0.54	0.033	0.012	8.18
Linewidth								
Cbla	55	0.392**	0.003	7.12	0.66	0.044	0.014	5.47
CSO	55	0.376**	0.005	5.00	0.44	0.028	0.009	4.99
HN	55	0.394**	0.003	5.58	0.72	0.048	0.015	7.37
Putamen	55	0.481**	0.000	6.82	0.56	0.048	0.012	6.22

Author Manuscript Author Manuscript Author Manuscript Author Manuscript

ROI	NAA			Intercept		Slope		Decade variation
	N	R	*p*	Value	SD	Value	SD	%
pWM	55	0.266 *	0.049	5.46	0.46	0.020	0.010	3.42
SCC	55	0.487 **	0.000	4.87	0.34	0.030	0.007	5.48
Thalamus	55	0.438 **	0.001	5.29	0.57	0.043	0.012	7.06

*Not significant but showing a tendency of age dependence ($0.008 < p < 0.05$)

**Significant linear correlation ($P < 0.008$) *Cbla* cerebellar anterior lobe, *MDd* midbrain tegmentum, *MDv* cerebral peduncle, *CSO* centrum semiovale, *fWM* frontal white matter, *HN* subcortical hand motor area, *iCap* posterior limb of the internal capsule, *pWM* parietal white matter, *SCC* splenium of the corpus callosum, *NAA* N-acetylaspartate and N-acetylaspartylglutamate, *Cho* choline-containing compounds, *tCr* creatine and phosphocreatine, *Glx* glutamate and glutamine, *mI* myo-Inositol

Clin Neuroradiol. Author manuscript; available in PMC 2021 September 01.